Ground-state phase diagram of an extended Hubbard chain with correlated hopping at half-filling

Liliana Arrachea,* E. R. Gagliano, and A. A. Aligia
Centro Atómico Bariloche and Instituto Balseiro, Comisión Nacional de Energía Atómica, 8400 Bariloche, Argentina
(Received 19 December 1995; revised manuscript received 18 April 1996)

We consider a generalized Hubbard model with on-site interaction U, nearest-neighbor repulsion V, and nearest-neighbor hopping for spin σ, which depends on the sum of particles $m_{\bar{\sigma}}$ with opposite spin in the two sites involved. The hopping matrix elements are denoted by t_{AA}, t_{AB}, t_{BB} for $m_{\bar{\sigma}}=0,1,2$, respectively. For $0<t_{AB}<t_{AA}=t_{BB}$, we have determined the regions of parameters for which the ground-state (GS) of the one-dimensional system is a charge-density wave (CDW), a spin-density wave (SDW), or a metal (M), using Hartree-Fock, exact diagonalization of finite chains and quantum Monte Carlo. The results agree qualitatively with the exactly solvable limit of $t_{AB}=0$. For $0<t_{AB}<t_{AA}=t_{BB}$, the GS is a M for sufficiently low values of U and V. In contrast, when $t_{AA}+t_{BB}-2t_{AB}=0$, our results suggest that the GS is either a CDW or a SDW, with the boundary between them lying near the line $U=2V$. [S0163-1829(96)08929-1]

I. INTRODUCTION

Two key physical ingredients, strong correlations and low dimensionality, seem to be crucial for the electronic structure of novel materials, such as the cuprate superconductors, quasi-one-dimensional organic conductors,[1] or conducting polymers.[2] The Hubbard model[3] is the generic model for interacting electrons in narrow-band and highly-correlated fermionic systems. It contains an *occupation-independent* nearest-neighbor hopping t and an on-site interaction U. However, in any physical realization, one would expect that the hopping energy depends on the occupation of the sites involved. In addition, in many real materials, particularly for low carrier densities or near a metal-insulator transition, there is considerable evidence that Coulomb interactions of longer range are essential, and one needs to include at least a nearest-neighbor repulsion V. This term allows one to obtain a correlation exponent $K_\rho<1/2$,[4] which seems necessary to explain the observed strong x-ray scattering at $4k_F$ in the organic compound TTF-TCNQ,[5] while in the Hubbard model $K_\rho \geqslant 1/2$ for all values of U/t.[6]

The above discussion leads naturally to the following Hamiltonian written in standard notation as

$$H=-\sum_{\langle ij\rangle\sigma}\phi_{ij}(c^{\dagger}_{i\sigma}c_{j\sigma}+\text{H.c.})+U\sum_i n_{i\uparrow}n_{i\downarrow}+V\sum_{\langle ij\rangle}n_i n_j, \tag{1}$$

where the correlated hopping ϕ_{ij} is given by

$$\phi_{ij}=\{t_{AA}(1-n_{i\sigma})(1-n_{j\sigma})+t_{BB}n_{i\sigma}n_{j\sigma}+t_{AB}[n_{i\sigma}+n_{j\sigma}-2n_{j\sigma}n_{i\sigma}]\}. \tag{2}$$

The particular case $V=0$ has been derived in different physical situations, as an effective one-band model to describe the low-energy physics of intermediate-valence systems,[7] ''hole'' superconductors[8] (including also phonons in the antiadiabatic approximation[9]), and cuprate superconductors.[10] Including V, the model contains the most important terms of the one-band Hamiltonian for the cuprate superconductors obtained by Schüttler and Fedro[11] and has been also proposed to describe the benzene molecule.[12]

The phase diagram has been investigated previously for $t_{AB}=0$ and also for $t_{AA}=t_{BB}=t_{AB}$ (Hubbard limit). In the first case, taking in addition $t_{AA}=-t_{BB}$, Strack and Vollhardt obtained the exact ground-state (GS) in arbitrary dimensions, in two regions of parameters using lower and upper bounds for the GS energy.[12] The lower bounds have been improved by Ovchinnikov.[13] The results have been extended to all values of t_{AA} and t_{BB} and the phase diagram has been determined exactly in one dimension (1D) for all (positive) values of U and V.[14] The results for $t_{AB}=0$ can be summarized as follows: in an arbitrary lattice in D dimensions with coordination number $z=2D$, the GS is a Mott insulator (MI), corresponding to all sites singly occupied, if

$$U>z\max(V,|t_{AA}|+|t_{BB}|). \tag{3}$$

This state possesses a high spin degeneracy. For $t_{AB}\neq 0$ the spin degeneracy is broken and this phase is a spin-density wave (SDW). For all simple cubic lattices and also other bipartite lattices like 3D bcc lattice,[15] the GS is a charge-density wave (CDW) if

$$V>\max(U/z,(U/2+|t_{AA}|+|t_{BB}|))/2. \tag{4}$$

For these lattices, in $D>1$, the GS possesses metallic behavior (M) within a region of (U,V) between these two phases. The exact boundary between M and MI is

$$U_{M-\text{MI}}=z(|t_{AA}|+|t_{BB}|). \tag{5}$$

The metallic character is not fully developed in $D=1$,[16] but the exact boundary between the gapless phase (M) and the MI is also given by Eq. (5).[17–19] Equation (5) is also valid for a 3D fcc lattice, a 2D hexagonal lattice, and other lattices[14,15] if $V=0$, $t_{AA}>0$, and $t_{BB}>0$.

Finally, for $D=1$, the boundary for $t_{AB}=0$ (Ref. 14) between the M and CDW is given by

$$V_{M-\text{CDW}}=(U/2+|t_{AA}|+|t_{BB}|)/2. \tag{6}$$

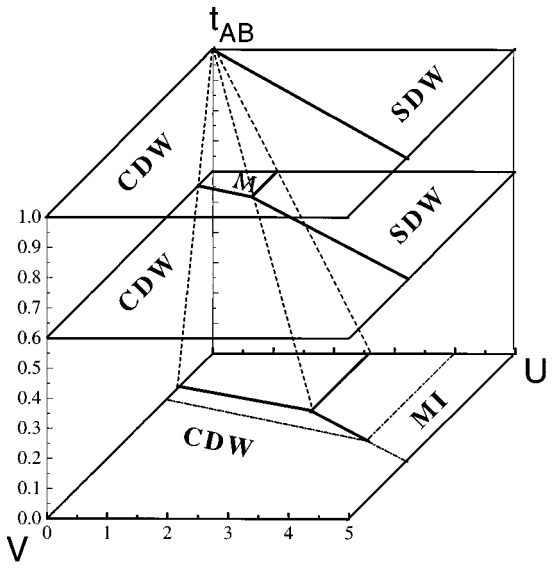

FIG. 1. Phase diagram of the one-dimensional extended Hubbard model with correlated hopping at half-filling for $t_{AA}=t_{BB}$ in the Hartree-Fock approximation. The solid lines in each plane $t_{AB}=$const separate the regions of charge-density-wave (CDW) and spin-density-wave (SDW) instabilities from the metallic (M) region (see text). The dashed lines, the line $U=V=0$, and the plane $t_{AB}=0$ delimit a pyramid inside which the system is metallic. The dashed-dotted lines correspond to exact boundaries for $t_{AB}=0$.

For $t_{AA}=t_{BB}=1$, the exact phase diagram in 1D is represented by the dashed-dotted line at the bottom of Fig. 1.

When $t_{AA}=t_{AB}=t_{BB}$ perturbation theory in high dimensions gives a boundary between the CDW and the SDW at $U=zV$ and no metallic phase.[20] In 1D, the phase diagram has been studied using the Hartree-Fock approximation,[21] real-space renormalization group,[22] Monte Carlo,[23] bosonization,[24,25] and exact diagonalization of finite chains.[26,27] All results coincide in that there is no M phase, except eventually, on the line of the second-order transition discussed below. The Hartree-Fock results (showed at the top of Fig. 1) predict a first-order transition between a CDW and a SDW again at $U=2V$. While these results are qualitatively correct, the other methods give a boundary slightly shifted to higher values of V, and obtain a continuous transition for small values of the interactions.[28] The line of the continuous transition ends at the tricritical point.[23–25,27] There is no overall agreement about the exact position of the tricritical point. Hirsch[23] located it at $U\sim 2V\sim 3t$, Cannon and Fradkin at $U\sim 2V\sim 1.5t$;[24] Cannon, Scalettar, and Fradkin at $U\sim 2V\sim(4-5)t$,[27] while Voit at $U\sim 2V\sim 4.76t$.[25] Our results suggest that the tricritical point might be located at $U\sim 2V\sim 4t$. We shall return to this point in Sec. VIII.

The aim of the present work is to determine, at least qualitatively, the 1D phase diagram in the space of the parameters (U,V,t_{AB}). We consider the third coordinate interpolating between both previously studied cases mentioned above. We remind the reader that due to the symmetry properties of the Hamiltonian,[15,29] changing the sign of all hoppings or that of t_{AB} alone, leads to an equivalent model. Thus we take $t_{AA}=1$ as the unit of energy and restrict to $t_{AB}\geqslant 0$. Interpolation between $t_{AA}=t_{AB}=t_{BB}$ and $|t_{AA}|-|t_{BB}|=t_{AB}=0$ can be done in two nonequivalent ways, depending on the sign of $t_{AA}t_{BB}$ in the exactly solvable limit: (a) keeping $t_{AA}=t_{BB}$, (b) keeping $t_{AA}+t_{BB}-2t_{AB}=0$ with $t_{AA}\neq t_{BB}$ [in this case, the three-body term of the Hamiltonian Eqs. (1) and (2), vanishes[8,29]]. We have studied both cases using the Hartree-Fock approximation, quantum Monte Carlo, and exact diagonalization. The results are qualitatively radically different in both cases. For the sake of clarity we show in Fig. 1, the Hartree-Fock phase diagram for the case (a). The volume inside the pyramid corresponds to the metallic (M) phase. In case (b) the M phase shrinks to the line $U=V=0$. In Sec. II we explain the Hartree-Fock approximation. Sections III and IV contain a description of the numerical methods and technical details. Sections V and VI contain the results for CDW and SDW order parameters obtained using Monte Carlo and the Lanczos method. Section V studies the CDW-SDW transition, while Sec. VI refers to the metal-insulator transitions M-SDW and M-CDW. Section VII is an analyzes the peaks at incommensurate wave vectors of the correlation functions in the metallic phase. Section VIII is a summary and discussion.

II. HARTREE-FOCK PHASE DIAGRAM

To treat Eq. (1) within the Hartree-Fock approximation, it is useful to separate the zero-, one-, and two-body contributions of the correlated hopping term as

$$\phi_{ij}=t_1+t_2(n_{i\bar{\sigma}}+n_{j\bar{\sigma}})+t_3 n_{i\bar{\sigma}}n_{j\bar{\sigma}}, \tag{7}$$

where

$$t_1=t_{AA},\ \ t_2=t_{AB}-t_{AA},\ \ t_3=t_{AA}+t_{BB}-2t_{AB}. \tag{8}$$

We consider solutions with broken symmetry in a simple cubic lattice of D dimension to describe the SDW and CDW phases. The order parameters for these phases, defined by Eq. (9), are the staggered magnetization m, for the SDW phase, and n, for the CDW one. The mean values of the occupations in real space are functions of them as follows:

$$n_{i\sigma}^{\mathrm{SDW}}=\tfrac{1}{2}[1+\sigma m\exp(i\mathbf{Q}\cdot\mathbf{R_i})],$$

$$n_{i\sigma}^{\mathrm{CDW}}=\tfrac{1}{2}[1+n\exp(i\mathbf{Q}\cdot\mathbf{R_i})], \tag{9}$$

where $\mathbf{Q}=\boldsymbol{\pi}$. The decoupling of the two- and three-body terms has been made as in Ref. 7. The Hartree-Fock Hamiltonian results

$$H_{\mathrm{HF}}=E+\sum_{k\sigma}[(-\overline{t\epsilon}_k+U_0)c_{k\sigma}^{\dagger}c_{k\sigma}+U_Q^{\sigma}c_{k\sigma}^{\dagger}c_{k+Q\sigma}], \tag{10}$$

where

$$A=\frac{1}{L}\sum_k \epsilon_k\langle c_{k\sigma}^{\dagger}c_{k\sigma}\rangle,\ \ \epsilon_k=2\sum_i^D\cos(k_i)$$

$$U_0=\frac{U}{2}-2t_2A-t_3A+2V \tag{11}$$

and for the SDW phase,

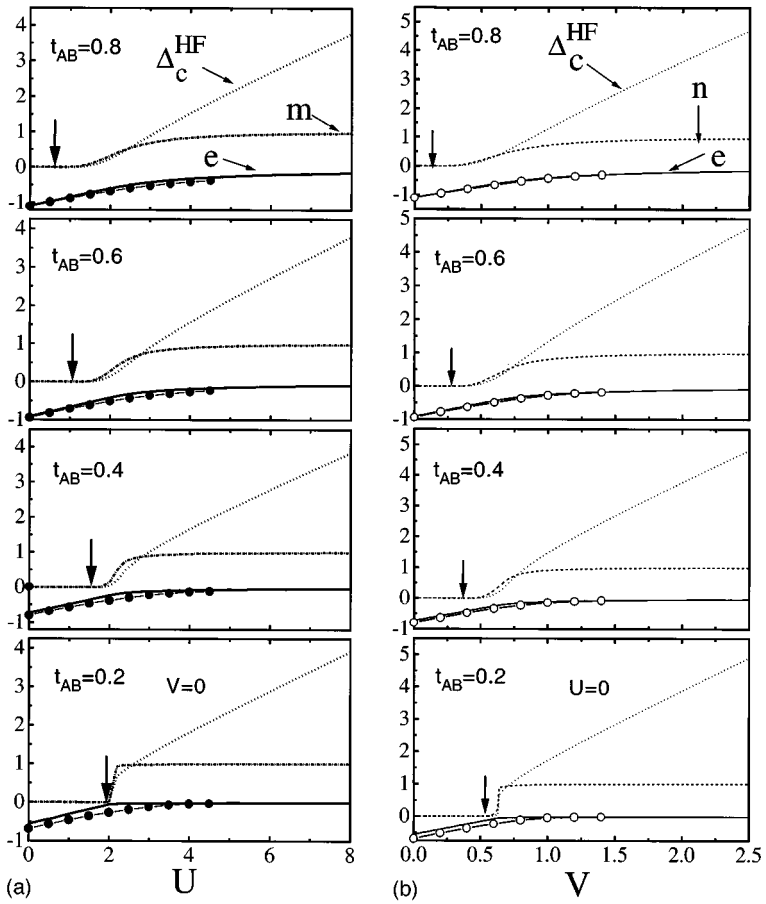

FIG. 2. Hartree-Fock results for the ground state energy per site e (solid line), SDW (left) or CDW (right) order parameter (dashed line), and charge gap Δ (dotted line) as a function of U at $V=0$ (left) or V at $U=0$ (right) for several values of t_{AB}. Open circles are exact results from ED on a $L=12$ ring. Vertical arrows indicate where a nonvanishing charge gap sets in.

$$\overline{t}=t_1+t_2 n+t_3\tfrac{1}{4}[(1-m^2)-3A^2]+\tfrac{1}{2}VA$$

$$U_Q^\sigma=-\sigma m\left[\frac{U}{2}-t_3 A\right],$$

$$E=2A\left[t_2+t_3\frac{(1-m^2-A^2)}{2}\right]-\frac{U}{4}(1-m^2)+V(\tfrac{1}{2}A^2-1), \tag{12}$$

while for the CDW one,

$$\overline{t}=t_1+t_2 n+t_3\tfrac{1}{4}[(1-n^2)-3A^2]+\tfrac{1}{2}VA$$

$$U_Q^\sigma=-n\left[2V-\frac{U}{2}-t_3 A\right],$$

$$E=2A\left[t_2+t_3\frac{(1-n^2-A^2)}{2}\right]-\frac{U}{4}(1+n^2)$$

$$+V\left[\frac{1}{2}A^2-(1-n^2)\right]. \tag{13}$$

The gap in both phases is $\Delta=|U_Q^\sigma|$. For $V=0$ we find a nonzero solution for the gap Δ^{SDW} when $U<U_c$, with

$$U_c=t_3\frac{4}{\pi}, \tag{14}$$

in 1D. It is easy to see that this boundary between the metallic phase and the SDW one ($U>U_c$) is not affected by the addition of a small nearest-neighbor Coulomb repulsion V. The gap equation for the CDW solution Δ^{CDW} possesses nonzero solution for $V>V_c$, with

$$V_c=t_3\frac{1}{\pi}+\frac{U}{4}, \tag{15}$$

in 1D. The critical values, Eqs. (14),(15), are $4/\pi$ times smaller than those obtained in 2D. Finally, for $U>U_c$, the boundary between the CDW and the SDW is given by $V=U/2$, as in the Hubbard limit. These boundaries are shown in Fig. 1, for particular values of t_{AB} with $t_{AA}=t_{BB}=1$. In Fig. 2, the values of the energy for different values of t_{AB}, are compared with those obtained by numerical diagonalization of finite chains. We find quantitative agreement for $t_{AB}\gtrsim 0.5$, for all values of the other parameters. For smaller values of t_{AB}, the agreement with the results of exact diagonalization of finite chains is not so good for $V<V_c$, where $\Delta^{\mathrm{CDW}}=0$. For strictly $t_{AB}=0$ and $U>U_{M-\mathrm{MI}}$ [see Eq. (5)], the ground state is a spin-degenerate Mott insulator.[14,18] However, a nonzero but small t_{AB} introduces an effective nearest-neighbor exchange interaction $J=4t_{AB}^2/(U-V)$, and the antiferromagnetic correlations and with it the SDW phase is restored. It can be seen in Fig. 1 that even in this limit, the SDW Hartree-Fock approximation gives qualitatively well the boundaries between the different phases. This is due to the fact that although true long-range order does not exist in the chain, the antiferromagnetic Hartree-Fock solution describes well the exact short-range order.

III. NUMERICAL METHODS AND TECHNICAL DETAILS

The properties of the 1D electron gas have been extensively studied in the past by using a weak-coupling g-ology scheme.[30] This approach provides important insight for the characterization of the ground state properties of one-dimensional correlated systems. In particular, it suggests that the competing phases with true long-range order are limited to charge-density waves (CDW), bond-ordering waves (BOW), and phase separation (PS). Power law decaying correlation functions are expected to occur in the metallic regime as well as in the spin-density-wave (SDW) phase.

Two complementary numerical algorithms have been used to investigate the properties of the 1D generalized Hubbard model, exact diagonalization (ED) of small clusters by the Lanczos algorithm, and the quantum Monte Carlo technique (QMC). Because ED methods are restricted to small clusters, we need to choose properly the boundary conditions in order to reduce as much as possible finite-size effects and have a smooth behavior of static properties as a function of band-filling $\rho=N_e/L$, where N_e is the number of particles and L is the chain length. The boundary condition at the closing link renormalizes the hopping amplitude $t\rightarrow te^{iL\phi}$, so the system is not translation invariant. However, redefining the fermion operators by attaching a piece of flux to each of them, one can recover translation invariance. The background flux per link ϕ originates from the boundary conditions and can be fixed by general considerations. In fact, if there is no external field, the ground state of a system with an even number of particles will have no net current flow. Hence, ϕ must satisfy $\langle\psi_0|J(\phi)|\psi_0\rangle=0$, where $|\psi_0>$ is the ground state wave function and J is the current operator. For noninteracting fermions with spin, one can do the calculation analytically and find that ϕ is 0 for $N_e=4m+2$ (periodic boundary conditions) and π/L for $N_e=4m$ (antiperiodic boundary conditions), where m is an integer number. For the interacting case, we checked numerically that this choice is also appropriate. Quite generally, after this choice of the background flux, the ground state energy behaves smoothly as a function of $1/L$.

For QMC calculations, we implemented the world-line algorithm as described in Ref. 31. We make use also of the plaquette representation of Ref. 32. Since we are interested in GS properties, the temperature was chosen in order to reach the GS plateau.[33] Most of the simulations were carried out on systems of up to 64 sites at inverse temperatures of $\beta=20$. The Trotter time step $\Delta\tau$ was fixed at 0.125. A typical simulation involved (5–55) K warm-up and (150–800) K sweeps through the lattice, with measurements performed every (5-8) sweeps and collected following a coarse-grained averaging procedure.[34] By contrast to the $t-U-V$ Hubbard model, simulations of the generalized model Eq. (1) at low temperatures are quite demanding due to near degeneracies in the low-energy part of the spectrum for particular values of the hopping parameters. These almost degenerate states show up, for example, at $t_{AA}=t_{BB}=1$ as $t_{AB}\rightarrow 0$. Complete degeneracy is found at $t_{AB}=0$. This is related with the conservation of the number of double occupied sites d. In this case, for $U<U_{M-\mathrm{MI}}$ [see Eq. (5)], there exists a finite density of doublons $\rho_d=d/L$, which varies continuously between $\rho_d=0.25$ $(U=0)$ to $\rho_d=0$ $(U\geq U_{M-\mathrm{MI}})$. The doublons, as well as the holes, move through the lattice interchanging their positions with the $L-2d$ unpaired spins. The total kinetic energy is equal to that of $L-2d$ spinless fermions.[17–19] In a finite-size lattice, the number of doublons in the GS, d_0, changes discontinuously as a function of U, but there is a large number of excited states with d near d_0. For example, the excited states for which $d=d_0\pm 1$, have an excitation energy $\sim -4t\cos(k_F^{\mathrm{sp}}\mp 2\pi/L)\pm U$ with $k_F^{\mathrm{sp}}=\pi(1-2d_0/L)$. In addition, for $t_{AB}\rightarrow 0$ and fixed d, there is a large spin and pseudospin degeneracy (the latter related with permutations of doublons and holes[17–19]) which for an open chain amounts to $2^{L-2d}\binom{2d}{d}$.[18]

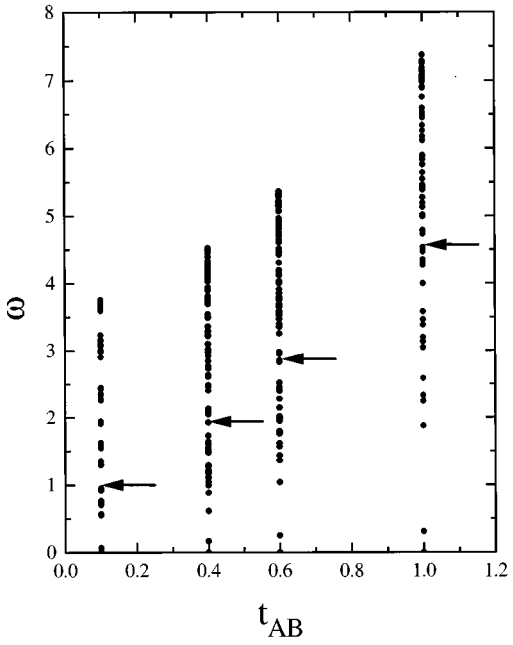

FIG. 3. Energy relative to the ground-state energy of the first 100 lowest states of a $L=8$ generalized Hubbard ring at half-filling for total wave vector $k=0$, $t_{AA}=t_{BB}=1$, $U=3$ and different values of t_{AB}. The arrows indicate the position of the 24th level.

At finite $0\leq t_{AB}\leq 0.5$, the conservation of d is almost fulfilled and the low energy levels have an approximately well defined number of doublons. In Fig. 3, we show the energy spectrum at half-filling for an 8-site ring with periodic boundary conditions in the sector of total wave vector $K=0$ for some values of t_{AB}. It is clearly seen that as $t_{AB}\rightarrow 0$, the low energy part of the spectrum is more dense than in the Hubbard case. At $t_{AB}=0.1$ and $U=3$, the ground state has $d\sim 1$. There is a small gap $\Delta\sim 0.14$ between the GS and the first excited state with $d\sim 0$. Higher excited states have either $d\sim 0$ or $d\sim 1$.

For small t_{AB} and V, and values of U corresponding to the metallic phase, but near the boundary with the SDW insulating phase, we were not able to reach the ground-state energy (known from Lanczos in small rings or from exact results for $t_{AB}=0$) with QMC, even doing simulated annealing. The cause of this failure might be ascribed to the following fact: In each QMC sweep, the world lines are deformed by means of *local* changes in the $(1+1)$ lattice. When a doublon and an empty site meet at nearest-neighbor sites, the algorithm always replaces them by two nearest-neighbor singly occupied sites because of the local gain in energy

$U-V$, while the opposite process, although favored by the kinetic energy, should overcome a large energy barrier. This situation has some similarities with the usual $t-U$ Hubbard model for large U, which was solved by a *simultaneous* deformation of spin-up and down world lines. We were not able to find a similar special update for our problem. So, after warm up, we equilibrate in one of the so many states close to the GS with $d=0$ and never reach the *zero-temperature plateau*.

The ''almost conservation'' of d for small t_{AB} has also consequences in the ED analysis. For example, in the limit of $t_{AB}=V=0$ and for $U<U_{M-\mathrm{MI}}$, the density of doublons in the thermodynamic limit ρ_d is known. For some finite systems, it can happen that $L\rho_d$ is not an integer, the Lanczos method chooses one (or both) of two integer values of d nearer to $L\rho_d$, and this introduces a nonmonotonic dependence of the physical quantities with size.

To study the properties of the generalized Hubbard model we first performed ED calculations of the charge gap $\Delta=E_0(N_e+1)+E_0(N_e-1)-2E_0(N_e+1)$ for different system sizes. $E_0(N_e)$ is the ground state energy of a system with N_e particles. Next, we calculate the charge $C(q)$ and spin $S(q)$ structure factors by ED and QMC methods. These structure factors are defined as the Fourier transform of the charge-charge and spin-spin spatial correlation functions,

$$C(q)=\frac{1}{L}\sum_{i,j}^{L}\langle(n_{i\uparrow}+n_{i\downarrow})(n_{j\uparrow}+n_{j\downarrow})\rangle e^{iq(i-j)}, \qquad (16)$$

where $q=(2\pi/L)\,n$ and $n=0,1,\ldots,L-1$,

$$S(q)=\frac{1}{4L}\sum_{i,j}^{L}\langle(n_{i\uparrow}-n_{i\downarrow})(n_{j\uparrow}-n_{j\downarrow})\rangle e^{iq(i-j)}. \qquad (17)$$

In the QMC simulations, we have also collected $\sim 32\,000$ partial averages of the order parameters,

$$m=\tfrac{1}{2}\sum_{i}(-1)^i\langle n_{i\uparrow}-n_{i\downarrow}\rangle,$$

$$n=\tfrac{1}{2}\sum_{i}[1+(-1)^i\langle n_{i\uparrow}+n_{i\downarrow}\rangle], \qquad (18)$$

corresponding respectively to the SDW and CDW phases. For further characterization of these phases, we built up histograms of these quantities.

IV. HOW TO DETECT THE SDW AND CDW REGIONS?

At $q=\pi$, $S(q)$ and $C(q)$ can be used to identify the CDW and SDW phases. In fact, in a perfect CDW or Neel state $C(\pi)$ or $S(\pi)$ diverge as $L\to\infty$. However, because in 1D there is no true magnetic long-range order, $C(\pi)$, in the CDW region, diverges faster than $S(\pi)$ for the SDW phase, when the length of the cluster is increased. In fact, in a perfect CDW, $C(\pi)\sim L$, while in the strong coupling limit $U\gg t$, $S(\pi)\sim(\ln L)^{1+\sigma}$ with $0.2<\sigma<0.3$.[35] $C(\pi)$ $[S(\pi)]$ is expected to sature or decrease with size if the system is not in a CDW (SDW) state.

The information given by the histograms of the order parameters Eq. (18) is also very useful to determine not only the boundary of the CDW and SDW phases, but also to distinguish between a first order and a continuous transition.[23,24] In the finite system, these histograms provide a direct measure of the probability distribution (PD) associated to quantum fluctuations. In a disordered phase, the PD exhibits a maximum around zero, which sharpens as $L\to\infty$. In contrast, in a SDW (CDW) phase the PD of $m(n)$ is characterized by two absolute maxima located at $\pm m_0$ $(\pm n_0)$, which also sharpen as L is increased. When a transition boundary is approached from the ordered phase, the shape of the PD of the corresponding order parameter gives information about the nature of the transition. In a continuous transition, the two maxima of the PD in the ordered phase evolve smoothly to a single one by crossing the boundary line. In a first order transition, the two maxima of the ordered phase show up as metastable (not absolute) ones outside this region. This gives rise to hysteretical behavior of measured quantities.[23] This type of analysis has been done for the SDW-CDW transition of the $t-U-V$ model[23,24] and is similar to the one proposed in Ref. 36 for finite-temperature phase transitions.

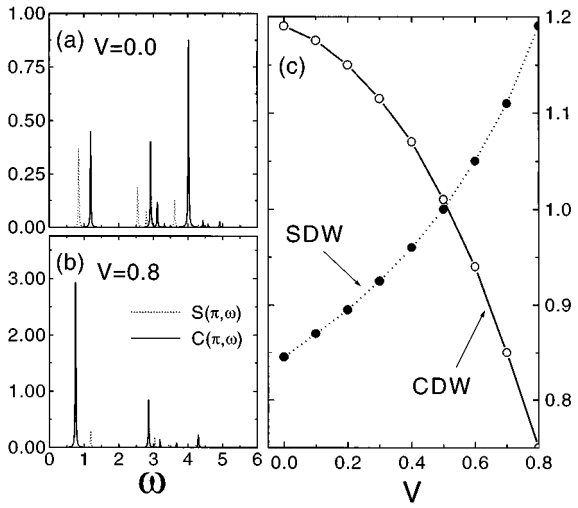

FIG. 4. Spin (dotted line) and charge (solid line) dynamical structure factors at $U=1$ for the $t-U-V$ model in a ring of $L=12$ sites. (a) $V=0$ (SDW phase) and (b) $V=0.8$ (CDW phase). (c) spin and charge lowest energy excitations of wave vector $q=\pi$ as a function of V.

Complementary, ED calculations can be also helpful in determining the CDW-SDW boundary line. In what follows, we describe our approach for this case. In a finite-size cluster, there can be no spontaneous symmetry breaking. A two-fold degenerate ground state such as the CDW state in an infinite lattice will be detected as two nearly degenerate states in a finite size cluster. These states will have opposite parity, a result which can be used in finite-cluster calculations to estimate the location of the transition boundary line. To illustrate this feature, let us consider a cluster of only two-sites in the $t-U-V$ model. In this system, the ground state wave function is a combination of a $S=0$ CDW- and a $S=0$ SDW-like states. By application of the *staggered* charge or magnetization order parameters, this state is connected to triplet excited states with $q=\pi$. These excitations can be characterized as triplet CDW- and SDW-like states.

The spin $S(q,\omega)$ and charge $C(q,\omega)$ dynamical structure factors will detect these excitations at low frequencies and the SDW-CDW transition will be the result of a level crossing between the lowest excitations on both sectors. For the case of $L=2$ and $L=4$, ED calculations locate the crossover at $U=2V$ in agreement with the change of the weight of the states with maximum order parameter in the exact analytical solution of these clusters. For other cluster sizes, we perform ED numerical calculations. In Figs. 4(a,b), we plot $S(\pi,\omega)$ and $C(\pi,\omega)$ well inside the SDW and CDW phases for $L=12$. The lowest-energy peak corresponds to the spin-spin and charge-charge correlations for $V=0$ and $V=0.8$, respectively. Following these excitations as a function of V, we were able to locate the SDW-CDW ''transition'' point, which for $U=1$ is at $V\sim 0.51$, in good agreement with previous calculations. Higher energy states of these spectra correspond to multimagnon and charge excitations which are well separated from the low energy peaks.

V. SDW-CDW BOUNDARY LINE

In this section we will examine the competition between CDW long-range and SDW algebraic order for both cases: (a) $t_{AA}=t_{BB}$ and (b) the electron-hole asymmetric case $t_{AA}+t_{BB}-2t_{AB}=0$. We have calculated the CDW and SDW structure factors on rings of up to 64 sites by using QMC techniques and up to 12 sites by using ED methods to identify these regions of the $(t_{AB}-U-V)$ phase diagram for the half-filled case.

A. Symmetric case

In this case we fix $t_{AA}=t_{BB}=1$ and change t_{AB} from 0 to 1. As explained in Sec. I, this study of the electron-hole symmetric case provides an interpolation between two previously solved cases, namely the $t_{AB}=0$ plane and the $t-U-V$ model. Aside from the trivial case of $U=V=0$ for which the system is metallic, the CDW and SDW regions are the only possible phases for positive values of the Coulomb interaction parameters in the $t_{AB}=1$ plane. By contrast, three competing phases exist for $t_{AB}=0$: CDW, metallic, and the Mott-insulating regime. As already stated, the GS is highly degenerate in the MI region where $U>2(|t_{AA}|+|t_{BB}|)$ and $V<U/2$. In particular, the perfect Néel and ferromagnetic states are part of the spin-degenerate GS. A small hopping t_{AB} breaks this degeneracy in favor of a SDW state. Clearly at large V, this hopping process amounts only to a diagonal correction $-2t_{AB}^2/(3V-U)$ to the energy of the CDW state with maximum order parameter. Thus the CDW region will be not very much affected as $t_{AB}\to 1$. In Fig. 5, we show the spin and charge structure factors for $t_{AB}=0.6$ and $U=1$. This value of U is very close to the boundary between the SDW and the M phases, predicted by the Hartree-Fock method ($U_c=1.02$ for this value of t_{AB}). These structure factors have the same shape that we find for the $t-U-V$ model for the same value of U. In the present case, $S(\pi)$ seems to have a stronger divergence for the smaller values of $V<U/2$ than that observed in the $t-U-V$ limit. However, it is not obvious that the system is within the SDW phase for this value of U. We shall return to this point in the next section. At large values of $V>U/2$, the system is characterized by $2k_f$ CDW

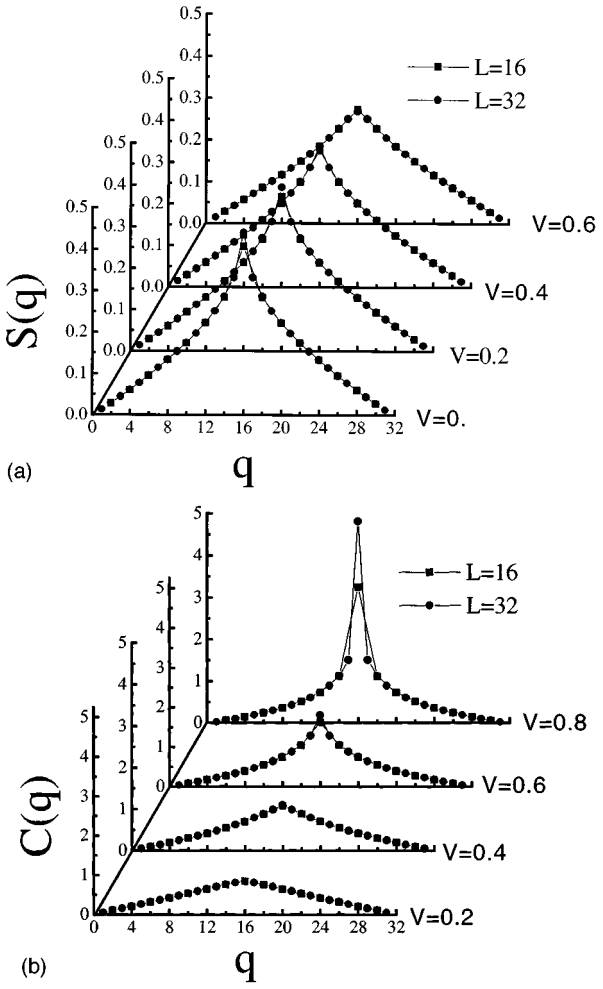

FIG. 5. (a) Spin-spin and (b) charge-charge structure factors of the half-filled generalized Hubbard model at $U=1.0$, $t_{AB}=0.6$, and $L=16,32$. The wave vector q is measured in units of $\pi/16$.

correlations. As V is decreased, $C(\pi)$ decreases and at the same time, $S(\pi)$ gains intensity signaling dominating SDW fluctuations in the $V<U/2$ sector, while for small (large) values of V, the spin (charge) structure factor clearly increases with system size, indicating that the system is in the SDW (CDW) phase. Unfortunately, the value of V at the transition cannot be identified with enough accuracy neither with this method nor by the crossing of the lowest charge and spin excitations. The spin (charge) lowest excitation energy increases (decreases) monotonically with increasing V and for example, for $t_{AB}=0.6$ and $U=2.5$ they coincide at $V_c\sim 1.1$. Although in the $t-U-V$ model, this approach works properly, in the present case V_c is too low, since one cannot expect a critical value smaller than that predicted by the Hartree-Fock calculation ($V\sim 1.25$). However, it shows indeed the softening of the CDW mode followed by an increase at larger V of $C(\pi)$ (from 0.07 at $V=1.0$ to 0.11 at $V=1.3$).

In Fig. 6, histograms of n, Eq. (18), are shown for $U=2.5$. The transition boundary is at $V\sim 1.27$, in good agreement with the Hartree-Fock results. The data of the histograms are nicely fitted by three Gaussians shown in the figure. One of them is centered around $n=0$, while the other two are centered around finite values $\pm n_0$. The three Gaus-

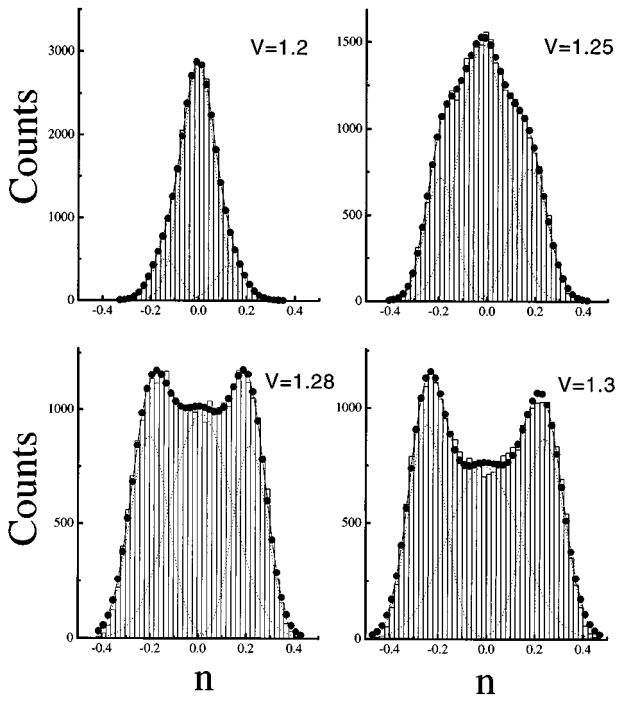

FIG. 6. Histograms of the CDW order parameter n in a $L=32$ site lattice for $t_{AB}=0.6$, $U=2.5$, and $V=0.12,0.125,0.128,0.13$.

sians reflect the fluctuations of the finite system between the two competing phases near the boundary line. The first one accounts for the weight of the fluctuations around states without CDW order in the total PD, while the latter correspond to the weight of fluctuations around ordered states, which gain intensity at expense of the former as the transition is approached. Interpolating the evolution of the three Gaussians between $V=1.25$ and $V=1.30$, we find a PD with three equal flat probability maxima separated by two shallow valleys, at $V=1.27$, what is a signal of a weak first-order transition. However, as found earlier,[24,27] the character of the transition is quite sensitive to finite-size effects. For example, it was found in the $t-U-V$ model, that for $V\lesssim 2$ the transition evolves from first to second order as the size of the system increases.[27] The position of the tricritical point will be discussed in Sec. VIII. The same behavior is obtained for other values of t_{AB} and for (U,V) outside of the pyramid drawn in Fig. 1. Inside the pyramid, the metallic phase is stabilized. Discussion about the CDW-M and SDW-M transition will be done in the next section.

For large values of the Coulomb interaction parameters, the SDW-CDW $U=2V$ transition line found for $t_{AB}=0$ is modified by this hopping process as a result of the effective exchange interaction $J\sim 4t_{AB}^2/(U-V)$ between neighboring spins in the SDW phase and the above mentioned second-order correction to the energy of the CDW state. The location of this boundary line can be estimated by equating the energy of the perfect CDW and SDW states including t_{AB} in perturbation theory as in Ref. 23. The resulting critical value of V is

$$V_c = U/2 + 1.545 t_{AB}^2/U. \tag{19}$$

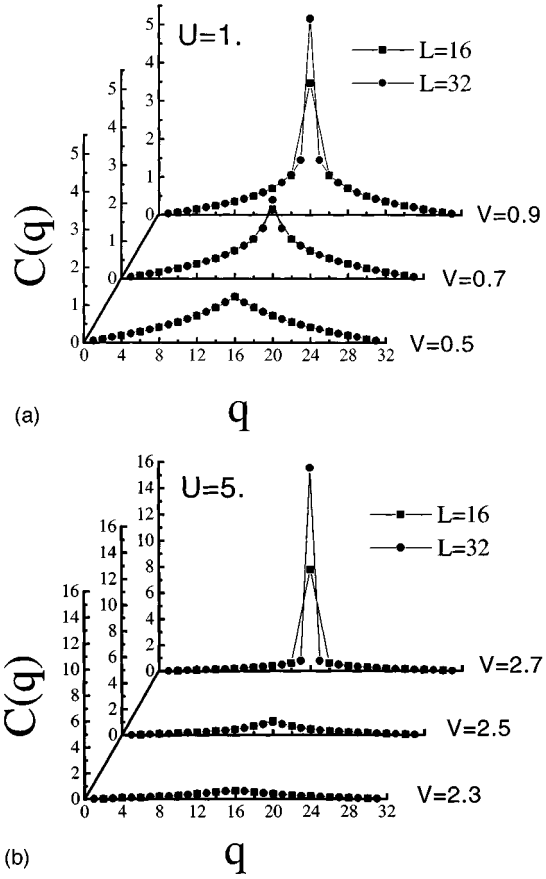

FIG. 7. Charge structure factor for the electron-hole asymmetric case, two system sizes, and (a) $U=1$ and (b) $U=5$. Other parameters are $t_{BB}=0.6$ and $t_{AB}=0.8$. The wave vector q is measured in units of $\pi/16$.

B. Asymmetric case

In this case, the two-body t_3 term does not contribute to the correlated hopping, see Eq. (6). The evolution towards the $t-U-V$ model can be thought as $-1\leqslant t_2\leqslant 0$. At $V=0$, depending on the value of t_{AB} (t_2), there are two distinct situations that one can find by rewriting Eq. (1) in k space. There is pairing between particles for $t_{AB}>t_{AA}$ $(t_2>0)$. Furthermore, numerical simulations and a BCS mean field calculation provide evidence in favor of a superconducting GS for small values of U.[8,29,37] Instead, in the Hartree-Fock approximation, the main effect of $t_2<0$ is to narrow the bandwidth. The gap equations (12) and (13) are the same as those of the $t-U-V$ model with a renormalized smaller hopping. Thus we do not find a gapless region in this case for any positive value of U and V. Therefore, the only possible phases correspond to SDW or CDW. In Fig. 7, we plot $C(q)$ for $U=1$ and $U=5$. We chose $t_{AA}=1$,$t_{BB}=0.6$, and $t_{AB}=0.8$ and perform calculations for $L=16$ and 32 using the QMC method. For $U=1$, the general behavior of $S(q)$ (not shown) is similar to that of Fig. 5(a). Instead, for $U=5$ and $V\leqslant 2.5$ $S(q)$ has the form of a sharp peak. Both structure factors peak at $q=\pi$. $C(\pi)$ increases as V is increased consistently with a transition to a CDW phase. At the same time, the behavior of $S(\pi)$ as a function of V is consistent with a SDW region at small V. At small U, the transition seems to be smooth while the structure factors at

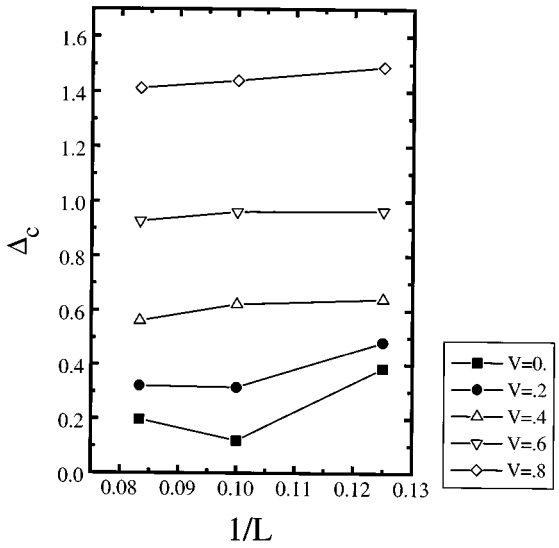

FIG. 8. Charge gap Δ_c vs inverse of system length for $t_{AB}=0.2$, $U=0$, and several values of V. For solid symbols, taken only the points with $L=8,12$ which have no frustration (see text in Sec. V) and assuming an error $\sim 5\%$ in Δ_c, the data are consistent with an extrapolation to $\Delta_c=0$ for $L\to\infty$.

$q=\pi$ change abruptly near the transition boundary for large values of the Coulomb interaction parameters [for $U=5$, $S(\pi)$ increases from ~ 0.18 to ~ 0.6 as U is decreased from 2.7 to 2.5]. For small values of U, the SDW-CDW transition line is as before, difficult to determine. However, for $U=5$, the size dependence of the structure factors clearly show that the critical value of V is near but slightly larger than $U/2$, in agreement with the strong-coupling value (19).

VI. THE METAL-INSULATOR TRANSITION

In the $t_{AB}=0$ plane, a whole gapless region appears at small values of U and V. As t_{AB} is turned on, the metallic phase in the Hartree-Fock solution decreases in size collapsing to one point $U=V=0$ in the $t_{AB}=1$ plane. To follow the M-CDW and M-SDW boundaries at finite t_{AB}, we calculate first the charge gap for different system sizes. In Fig. 8, we show our results for $t_{AB}=0.2$, and several values of V at $U=0$. For small values of $V<0.4$, we observed finite-size effects on systems of $4n+2$ sites due to frustration induced by the almost conservation of d for small values of t_{AB}. The optimum doublon density for $t_{AB}=V=0$ is $d/L=1/4$. A rough extrapolation of the gap suggest that the M phase extend up to $V\sim(0.2–0.4)$ to be compared with the Hartree-Fock value $V\sim 0.5$. For larger values of the nearest-neighbor Coulomb interaction, there are no noticeable frustration effects and the charge gap extrapolates to a finite value as $L\to\infty$. At the same time, the charge structure factor peaks at $q=\pi$ in the gapped region indicating the M-CDW transition. In Figs. 9(a,b), we plot $C(q)$ obtained by ED at $U=0$ for values of t_{AB} close to known limits ($t_{AB}=0$ and $t_{AB}=1$). In the CDW region, the peak at $q=\pi$ scales as L while in the metallic phase there is an incipient peak which signals only strong nearest-neighbor charge correlations rather than a true long-range order. According to the Hartree-Fock results [Eq. (14)], $V_c=0.51$ and $V_c=0.13$ for the values of t_{AB} and U

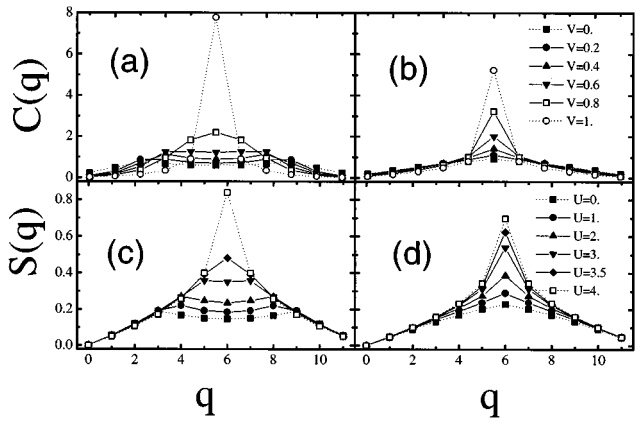

FIG. 9. Charge [(a) and (b)] and spin [(c) and (d)] structure factors of the half-filled generalized Hubbard model for a ring of $L=12$ sites, several values of V at $U=0$, and (a) and (c) $t_{AB}=0.2$, (b) and (d) $t_{AB}=0.8$. The wave vector q is measured in units of $\pi/6$.

used in Figs. 9(a) and 9(b), respectively. Near V_c, it seems that $C(q)$ is flat for $q\sim\pi$, while at least for small t_{AB}, if $V<V_c$, $C(q)$ peaks at incommensurate positions (discussed in the next section), while for $V>V_c$, the CDW peak at $q=\pi$ develops.

In Figs. 9(c,d), we show the spin structure factor $S(q)$ as a function of U for $V=0$ and the same values of t_{AB} as before. The Hartree-Fock critical value of U for these values is (c) $U_c=2.04$ and (d) $U_c=0.51$. As in the previous case, the shape of $S(q)$ changes near the M-SDW transition, but no clear criterion to determine the transition point can be established from the information gathered in Fig. 9.

We have also studied the scaling of the charge gap and Drude weight for different values of U and $V=0$. Δ_c decreases with increasing system size (like the behavior shown in Fig. 8 for $V=0.8$). All curves $\Delta_c(1/L)$ look very similar for $U<U_L$, while Δ_c increases with U for $U>U_L$. For $t_{AA}=t_{BB}=1$, $t_{AB}=0.6$, $U_L\sim 3.2$, considerably larger than the value U_c for which a gap opens according to the Hartree-Fock result Eq. (14). The Drude weight or charge stiffness is obtained from the flux dependence of the ground state energy (see Sec. III) as

$$D_c=\frac{L}{2}\left.\frac{\partial^2 E(L,\Phi)}{\partial\Phi^2}\right|_{\Phi=\Phi_0}. \tag{20}$$

For $t_{AA}=t_{BB}=1$, $t_{AB}=0.6$, the Lanczos results in systems of 4, 6, 8, 10, and 12 sites are consistent with an extrapolation to zero of D_c if and only if $U>3\sim U_L$, in agreement with the results of Δ_c. However, it is clear that the extrapolations to the thermodynamic limit are not valid if the correlation length ξ exceeds the size of our rings. For the Hubbard model ξ was calculated by Stafford and Millis and increases for decreasing U.[38] We interpret U_L as the minimum value of U for which the charge gap in the thermodynamic limit is of the order of the minimum possible charge excitation energy in our finite systems. It should be a lower limit to U_M, where $U_M\sim 2(t_{AA}+t_{BB})$ characterizes the crossover between two insulating regimes: a weak coupling one where

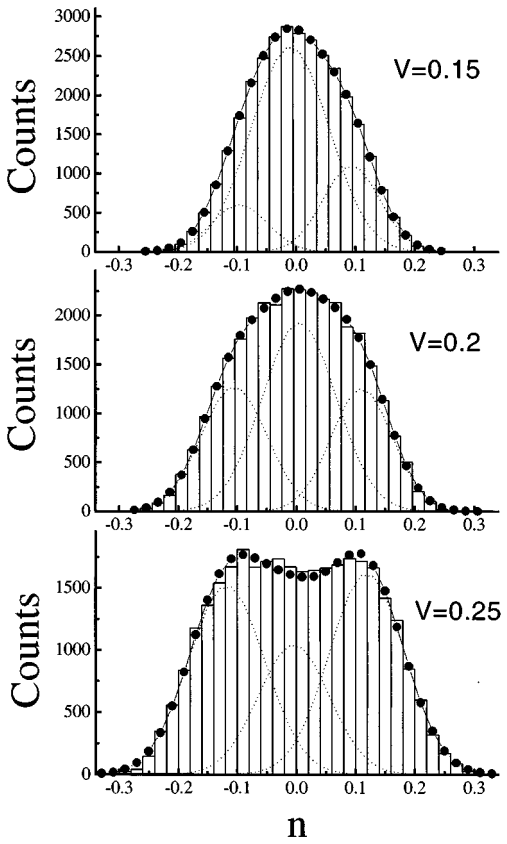

FIG. 10. Histograms of the CDW order parameter n in a $L=32$ site lattice for $t_{AB}=0.6$, $U=0$ and $V=0.15,0.2,0.25$. The curves have been fitted with three Gaussians, although they have not necessarily a physical meaning in this case.

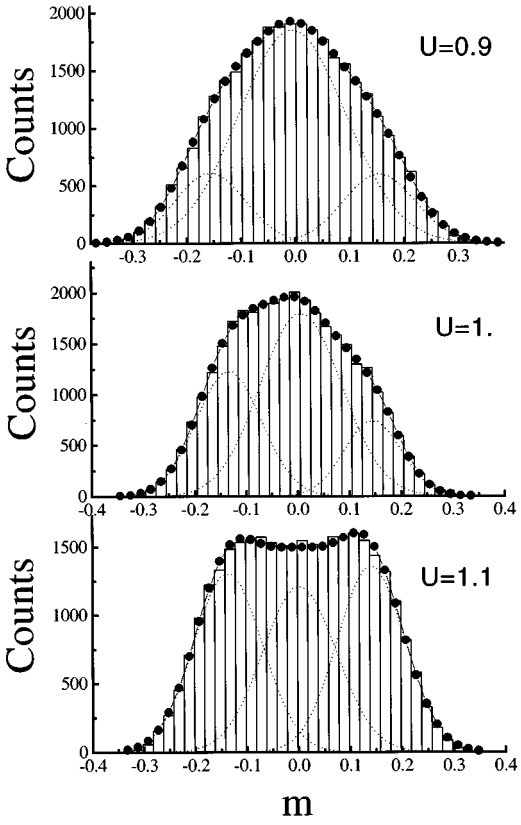

FIG. 11. Histograms of the SDW order parameter m in a $L=32$ site lattice for $t_{AB}=0.6$, $V=0$ and $U=0.9,1,1.1$. The curves have been fitted with three Gaussians, although they have not necessarily a physical meaning in this case.

the antiferromagnetic fluctuations introduced by t_{AB} and small U (combined with the nesting of the Fermi surface) open an exponentially small gap, and a Mott regime, in which the insulator has one (essentially) localized particle at each site.[18,39] Thus for $t_{AB}\neq 0$ a true Mott transition (from a metal to a Mott insulator) does not exist. Rather for small values of U ($\sim U_c$) a transition to a SDW takes place.

In our finite rings, we cannot detect the opening of a small SDW gap if it is smaller than the minimum possible charge excitation energy, which one can estimate as $2\pi/(Lv_c)$, where v_c is the charge velocity. However, the Mott regime is clearly identified. The charge velocity can be calculated in two ways. The more direct one uses the minimum energy as a function of wave vector $E_S(q)$, for the same total spin as the ground state[29]

$$v_c=\frac{E_S(2\pi/L+Q)-E_S(Q)}{2\pi/L}, \tag{21}$$

where S,Q are the total spin and wave vector of the ground state (both zero in our case). The other expression, valid when the system is in a Tomonaga-Luttinger-liquid regime is[29]

$$v_c^2=\frac{LD_c}{2}(E(N+2)+E(N-2)-2E(N)), \tag{22}$$

where $E(N)$ is the ground state of the ring with N particles. In an insulator, the concept of v_c becomes meaningless, and thus, a deviation of the results obtained using both expressions is again an indication of an opening of a (significant) charge gap. In rings from 8 to 12 sites, this deviation begins at $U\sim 1.5t$ for the Hubbard model and $U\sim 2.5$ if $t_{AA}=t_{BB}=1$, $t_{AB}=0.6$.

While neither the scaling of the charge gap or Drude weight, nor the study of the charge velocity in our small rings is able to detect the opening of an exponentially small gap, the position and character of the M-CDW and M-SDW transitions can be efficiently studied using the information obtained from the PD of the order parameters in the QMC calculations. In Fig. 10, results are shown for the PD of the CDW order parameter n at $U=0$ and $t_{AB}=0.6$ for an $L=32$ lattice. The transition from the metallic to the CDW phase takes place at $V\sim 0.25$, which is manifested by the development of two peaks in the PD. This is in good agreement with the Hartree-Fock prediction. From Fig. 11, a similar analysis can be made with m at $V=0$ to determine the transition from the metallic to the SDW. It seems to take place at $U\sim(1.00-1.10)$, also in agreement with Hartree Fock. In contrast to the results shown in Fig. 6, according to the PD (which shows one maximum evolving into two maxima with increasing values of the corresponding interaction), it is seen that both, the M-CDW and M-SDW are continuous transitions. This fact is also reflected in the behavior of the structure factors $C(q)$ and $S(q)$, which display

incipient divergences at $q=\pi$ within the M phase near the corresponding boundary. This is the case, for example, of $S(q)$ shown in Fig. 5(a) for small values of V. Our previous exact results for $t_{AA}=t_{BB}$, $t_{AB}=0$ have also led to continuous metal-insulator transitions.[14–16,18]

VII. SPIN-SPIN AND CHARGE-CHARGE CORRELATIONS IN THE METALLIC PHASE

As already mentioned in Secs. I and III, exact results for $t_{AB}=0$ (Refs. 12–19) show that the gapless phase (M) that exists for small U and V is characterized by large spin and charge degeneracies. It is interesting to study how the CDW and SDW correlations are introduced in the M phase as t_{AB} increases. We remarked in previous sections that for $t_{AB}\rightarrow 0$, doublons and holes can be almost identified as true particles. In dimensions higher than one,[14,15] these species introduce significant effects in the magnetic response. In particular, for $t_{AB}=0$ and $U\lesssim U_{M-\mathrm{MI}}$, where their concentrations are small, a double Nagaoka state with one hole and one doublon in a ferromagnetic background is expected. It is also rather likely that magnetic polarons of Nagaoka islands immersed in an antiferromagnetic background are formed for $t_{AB}\neq 0$.[15] In one dimension, the lattice does not fulfill the connectivity hypothesis of Nagaoka's theorem, so, in which way do the antiferromagnetic correlations grow as $t_{AB}\rightarrow 1$?

In the M phase, both structure factors display incommensurate responses with peaks at $q=\pi\pm\delta$, $\delta\rightarrow 0$ as $U\rightarrow U_c$, as is shown in Fig. 9. The shapes of $S(q)$ and $C(q)$ resemble the corresponding ones for the Hubbard model out of half-filling. To understand this result, let us consider first the limit $V=0$, $t_{AB}\rightarrow 0$. In this limit we have obtained that the ground state wave function can be factorized in three terms: one describing the position of the singly occupied sites, and the spin and pseudospin wave functions which describe respectively the spin of the unpaired particles and the charge in the remaining sites. This generalization of the wave function for the infinite U Hubbard model[40] has been proposed and verified by ED in Ref. 17. Because only unpaired fermions contribute to the spin structure factor, $S(q)$ does not depend on the pseudospin wave function. In particular if all doubly occupied sites are replaced by empty sites, we can take $S(q)$ from the result of Ogata and Shiba[40] for the $U\rightarrow\infty$ Hubbard model. Thus $S(q)$ is peaked at $q=\pi\rho_f$, where ρ_f is the density of unpaired fermions and is a simple function of $t_{AA}=t_{BB}$, U, and the total density $\rho=N_e/L$. For $t_{AA}=t_{BB}$, the transformation of Shiba[17,41] which interchanges empty sites with singly occupied sites with spin up, and doubly occupied sites with singly occupied sites with spin down, has the effect of changing the sign of U in the Hamiltonian. Using this transformation, at half-filling and for $q\neq 0$, we can write $C(q,1-\rho_f)=S(q,\rho_f)/4$. Thus the charge-charge correlation functions are peaked at $q=\pi(1-\rho_f)$ in the metallic phase of the system for $t_{AB}\rightarrow 0$.

For $t_{AB}\neq 0$, the number of doubly occupied and singly occupied sites are no longer conserved quantities. However, for small t_{AB}, the doublons (doubly occupied sites) and holes (empty sites) can still be thought as almost genuine particles and although $S(q)$ now changes if the doublons are replaced by holes, its qualitative behavior remains the same.

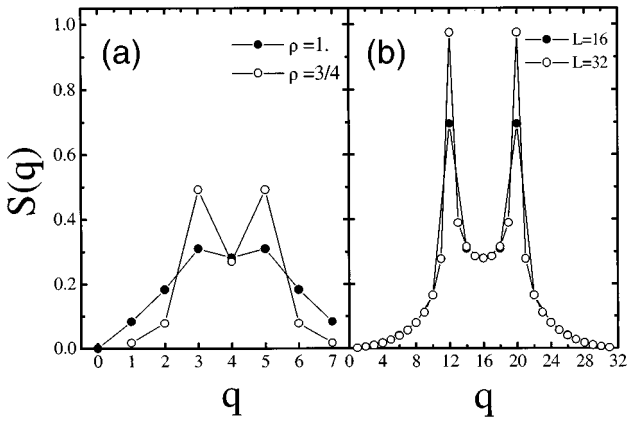

FIG. 12. Spin structure factor. (a) Obtained from ED for $L=8$ and two different densities. (b) Obtained from QMC for two different lengths and fixed density $\rho=3/4$. Other parameters are $t_{AB}=0.2, t_{AA}=t_{BB}=1, V=0, U=2.5$. The wave vector q is measured in units of $\pi/4$ in (a) and $\pi/16$ in (b).

This is an important fact from the practical point of view since the critical slowing down of our QMC treatment and the fact that the system is trapped in metastable states does not occur in the absence of doublons. In Fig. 12(a), we compare results of ED calculations of the spin-spin structure factor $S(q)$ at $t_{AB}=0.2$ and $U=2.5$, where $\rho_d=1/8$ before and after the replacement of the doublon by a hole. The main difference is found at small q where $S(q)\sim q^{\alpha}$ with $\alpha=1(2)$ for the doublon (two-hole) case. The incommensurate peak at $q=\pi\rho_f$ is seen in both cases, although there is no quantitative agreement. The intensity of the incommensurate peak increases as the system size is increased, as is shown in Fig. 12(b).

VIII. SUMMARY AND CONCLUSIONS

We have studied the phase diagram at half-filling of an extended Hubbard model which contains two physical ingredients expected to be important: the correlated hopping and the nearest-neighbor repulsion V. In addition to the charge-density-wave (CDW) and spin-density-wave (SDW) phases already known in the model without correlated hopping ($t-U-V$ model), there is also a metallic phase (M). The Hartree-Fock phase diagram shown in Fig. 1 is qualitatively correct for the $t-U-V$ model and an exactly solvable limit obtained previously. We have also studied the charge gap, charge-charge and spin-spin correlation functions, probability distributions of the order parameters of the CDW and SDW phases, and several aspects of the possible transitions as functions of the parameters of the model, using quantum Monte Carlo and exact diagonalization of finite rings. In spite of the difficulties of these methods (critical slowing down and finite-size effects), the results are consistent with the Hartree-Fock phase diagram. For small values of the interactions and small t_{AB} [see Eqs. (1) and (2)], the charge-charge and spin-spin correlation functions in the metallic phase are peaked at incommensurate wave vectors, even at half-filling.

We would like to discuss the nature of the transition between any two of the phases studied (CDW, SDW, M) and

the tricritical point for $t_{AA}=t_{BB}=t$ and $t_{AB}\leqslant t$. As discussed at the end of Sec. VI, the M-SDW and M-CDW transitions are continuous. For $t_{AB}=0$, the CDW-SDW transition, which takes place for $U>4t$ is discontinuous.[14] For small V, we also obtained in Sec. VI that the change of regime from a weak- to strong-coupling insulator takes place at some value $U_M>U_L\sim 2$. A similar effect is observed for small U in the CDW as V is increased. The value $U_M\sim 4t$ is consistent with previous studies of the position of the tricritical point for the $t-U-V$ model, which separates the line of second-order CDW-SDW transition at small U to that of first-order transition at large U.[23–25,27] In the renormalization-group schemes,[24,25] the criterion to determine the tricritical point is based on the change of the scaling dimension of an appropriate operator. Below the tricritical point, this operator is irrelevant indicating that the system is in a weak-coupling regime. These SDW and CDW weak-coupling regimes are strongly affected by t_{AB} and disappear in favor of a gapless metallic phase in the limit $t_{AB}\rightarrow 0$.

These facts, together with the results for $t_{AB}\rightarrow 0$ mentioned above, lead us to speculate that the tricritical point is located at $U=U_t\sim 4t$, almost independently of t_{AB}. Starting from the limit $t_{AB}=0$, it is clear that the effect of t_{AB} reduces the region of existence of the M phase, but one cannot expect that fluctuations induced by t_{AB} *increase* the region of first-order transition. Thus $4t$ should be a *lower bound* for U_t. The value of $U_t\sim U_M$ separates the weak coupling regime $U<U_t$ with a small gap which vanishes at the transition line, from the strong coupling regime $U>U_t$ with a large gap that cannot be reduced to zero by the combined effects of fluctuations introduced by t_{AB} and the competition between CDW and SDW. Therefore, the transition should be first order for $U\gg U_t$. Since the above arguments do not depend on dimensionality, one might expect the same qualitative behavior in dimensions $D>1$.

If finite-size effects were disregarded, the above considerations which places the tricritical point at $U\gtrsim 4t$ would be in clear contradiction with the Monte Carlo probability distribution results of Fig. 6, which are indicative of a first-order transition at $U\sim 2.5$. Cannon and Fradkin,[24] with the same method, also obtained first-order transitions at very low values of the interactions in the $t-U-V$ model. This was later ascribed to statistical errors, to large values of the time discretization ($\Delta\tau=0.5$), and to large temperatures.[27] Although all these features have been improved in the present study, we still find that it is necessary to do careful finite-size scaling for different values of the interactions, to be able to determine the position of the tricritical point by Monte Carlo or exact diagonalization of finite systems.[27]

If the three-body term of the correlated hopping vanishes [$t_3=0$ in Eq. (7)], the metallic phase disappears for the sign of the two-body term ($t_2<0$) considered here. However, previous numerical and mean-field calculations[8,29,37] show that for $t_3=0, t_2>0$, the system is superconducting, even at half-filling. Superconductivity also occurs for other parameters and fillings, like $t_{AB}<t_{AA}=t_{BB}, V=0$, small U, and out of half-filling.[17,29] Other interesting models with correlated hoppings also display superconductivity.[19,42,43]

ACKNOWLEDGMENTS

We thank E. Jagla for bringing Ref. 36 to our attention and discussions about it. We also thank Daisey Luz and R. R. dos Santos for helpful discussions. L.A. and E.G. were supported by CONICET. A.A.A was partially supported by CONICET. Partial support from Fundación Antorchas under Grant No. 13016/1 is gratefully acknowledged.

*Permanent address: Departamento de Física, Universidad Nacional de La Plata, 1900 La Plata, Argentina.

[1] D. Jérome and H. J. Schultz, Adv. Phys. **31**, 299 (1982).
[2] A. J. Heeger, S. Kivelson, J. R. Schriffer, and W. P. Su, Rev. Mod. Phys. **60**, 781 (1988).
[3] J. Hubbard, Proc. R. Soc. London Ser. A **276**, 238 (1963); M. C. Gutzwiller, Phys. Rev. Lett. **10**, 159 (1963); J. Kanamori, Prog. Theor. Phys. **30**, 275 (1963).
[4] H. Q. Lin, E. R. Gagliano, D. K. Campbell, E. H. Fradkin, and J. E. Gubernatis (unpublished).
[5] J. D. Pouget, *Highly Conducting Quasi-one-dimensional Crystal Semiconductors and Semimetals* (Pergamon, New York, 1988), Vol. 27, p. 87.
[6] H. Schultz, Phys. Rev. Lett. **64**, 2831 (1990).
[7] M. E. Foglio and L. M. Falicov, Phys. Rev. B **20**, 4554 (1979).
[8] F. Marsiglio and J. E. Hirsch, Phys. Rev. B **41**, 6435 (1990); references therein.
[9] F. Marsiglio and J. E. Hirsch, Phys. Rev. B **49**, 1366 (1994).
[10] M. E. Simón, M. Baliña, and A. A. Aligia, Physica C **206**, 297 (1993); M. E. Simón and A. A. Aligia, Phys. Rev. B **48**, 7471 (1993).
[11] H. B. Schüttler and A. J. Fedro, Phys. Rev. B **45**, 7588 (1992).
[12] R. Strack and D. Volhardt, Phys. Rev. Lett. **70**, 2673 (1993); references therein.
[13] A. A. Ovchinnikov, Mod. Phys. Lett. B **7**, 21 (1993).
[14] A. A. Aligia, L. Arrachea, and E. R. Gagliano, Phys. Rev. B **51**, 13774 (1995).
[15] E. R. Gagliano, A. A. Aligia, L. Arrachea, and M. Avignon, Phys. Rev. B **51**, 14012 (1995).
[16] When $t_{AB}=0$, the charge gap vanishes for small values of U and V. However, in 1D the Drude weight is always zero at half-filling (Refs. 14,17). In simple terms the system seems to be a a ''gapless semiconductor'' or a ''nonconducting metal.'' However, this feature is particular of the 1D topology and the conductivity is restored if $t_{AB}\neq 0$ or for a system of weakly coupled chains. Thus we shall refer to this phase as M in every case.
[17] L. Arrachea, A. A. Aligia, and E. R. Gagliano, Phys. Rev. Lett. **76**, 4396 (1996).
[18] L. Arrachea and A. A. Aligia, Phys. Rev. Lett. **73**, 2240 (1994).
[19] J. de Boer, V. E. Korepin, and A. Schadsneider, Phys. Rev. Lett. **74**, 789 (1995); A. Schadsneider, Phys. Rev. B **51**, 10386 (1995).
[20] P. G. J. Dongen, Phys. Rev. Lett. **67**, 757 (1991).
[21] D. Cabib and E. Callen, Phys. Rev. B **12**, 5249 (1975).
[22] B. Fourcade and G. Spronken, Phys. Rev. B **29**, 5089 (1984).
[23] J. E. Hirsch, Phys. Rev. Lett. **53**, 2327 (1984); Phys. Rev. B **31**, 6022 (1985).
[24] J. W. Cannon and E. Fradkin, Phys. Rev. B **41**, 9435 (1990).
[25] J. Voit, Phys. Rev. B **45**, 4027 (1992).
[26] B. Fourcade and G. Spronken, Phys. Rev. B **29**, 5096 (1984).

[27] J. W. Cannon, R. T. Scalettar, and E. Fradkin, Phys. Rev. B **44**, 5995 (1991).

[28] Strictly speaking, the real-space renormalization-group results (Ref. 22) give a smooth crossover between CDW and SDW with both order parameters different from zero near the ''transition'' line. Instead, the continuum field theory results (Refs. 24,25) give a second-order transition below a critical value of U, with both order parameters and the charge gap vanishing at the transition.

[29] L. Arrachea, A. A. Aligia, E. R. Gagliano, K. Hallberg, and C. Balseiro, Phys. Rev. B **50**, 16 044 (1994).

[30] J. Solyom, Adv. Phys. **28**, 201 (1979); J. Voit, Rev. Mod. Phys. (to be published).

[31] J. E. Hirsch, R. L. Sugar, D. J. Scalapino, and R. Blankenbecker, Phys. Rev. B **26**, 5033 (1982); J. E. Hirsch, D. J. Scalapino, R. L. Sugar, and R. Blankenbecler, Phys. Rev. Lett. **47**, 1628 (1981).

[32] W. R. Somsky and J. E. Gubernatis, Comput. Phys. **6**, 178 (1992).

[33] In a finite-size system, the mean value of any observable is given at large β by $\langle A\rangle\sim\langle \mathrm{GS}|A|\mathrm{GS}\rangle+\langle 1\mathrm{st}|A|1\mathrm{st}\rangle\exp[-\beta(E_1-E_0)]$, where E_0 and E_1 are the energies of the ground state (GS) and first-excited state (1st), respectively. For temperatures satisfying $\beta\gg 1/(E_1-E_0)$, $\langle A\rangle\sim\langle$ GS$|A|$GS$\rangle$ and we refer to those temperature values as the zero-temperature plateau.

[34] W. W. Wood, in *Physics of Simple Liquids*, edited by N. V. Temperley, J. S. Rowlinson, and S. S. Rushbrooke (North-Holland, Amsterdam, 1968), Chap. 5.

[35] K. Kubo, T. A. Kaplan, and J. R. Borysowicz, Phys. Rev. B **38**, 11550 (1988).

[36] A. Ferrenberg and R. H. Sweden, Phys. Rev. Lett. **53**, 2327 (1984); J. Lee and J. M. Kosterlitz, *ibid.* **65**, 137 (1990).

[37] G. Japaridze and E. Müller-Hartmann, Ann. Phys. (N.Y.) **3**, 163 (1994); M. Airoldi and A. Parola, Phys. Rev. B **51**, 16327 (1995).

[38] C. A. Stafford and A. J. Millis, Phys. Rev. B **43**, 13660 (1991); **48**, 1409 (1993).

[39] P. Nozieres, Ann. Phys. (France) (to be published).

[40] M. Ogata and H. Shiba, Phys. Rev. B **41**, 2326 (1990).

[41] H. Shiba, Prog. Theor. Phys. B **48**, 2171 (1972).

[42] G. Santoro, M. Airoldi, N. Manini, E. Tosatti, and A. Parola, Phys. Rev. Lett. **74**, 4039 (1995).

[43] C. D. Batista, F. Lema, and A. A. Aligia, Phys. Rev. B **52**, 6223 (1995).